

## Supporting Information

### **A $\text{LiPF}_6$ -Electrolyte-Solvothermal Route for the Synthesis of $\text{LiF/Li}_x\text{PF}_y\text{O}_z$ -Coated Li-rich Cathode Materials with Enhanced Cycling Stability**

Chaochao Fu<sup>\*a</sup>, Jiayun Wang<sup>a</sup>, Jinfeng Wang<sup>a</sup>, Linglong Meng<sup>a</sup>, Wenming Zhang<sup>\*b</sup>, Xiaoting Li<sup>\*a</sup>, and Liping Li<sup>\*c</sup>

<sup>a</sup>National & Local Joint Engineering Research Center of Metrology Instrument and System, College of Quality Technology Supervision, Hebei University, Baoding 071002, P.R. China.

E-mail: [ccfu@hbu.edu.cn](mailto:ccfu@hbu.edu.cn) (C. Fu); [lxt@hbu.cn](mailto:lxt@hbu.cn) (X. Li)

<sup>b</sup>Hebei Key Lab of Optic-electronic Information and Materials, College of Physics Science and Technology, Hebei University, Baoding 071002, P.R. China. E-mail: [wmzhanghbu@126.com](mailto:wmzhanghbu@126.com) (W. Zhang)

<sup>c</sup>State Key Laboratory of Inorganic Synthesis and Preparative Chemistry, College of Chemistry, Jilin University, Changchun 130012, P.R. China. E-mail: [lipingli@jlu.edu.cn](mailto:lipingli@jlu.edu.cn) (L. Li)

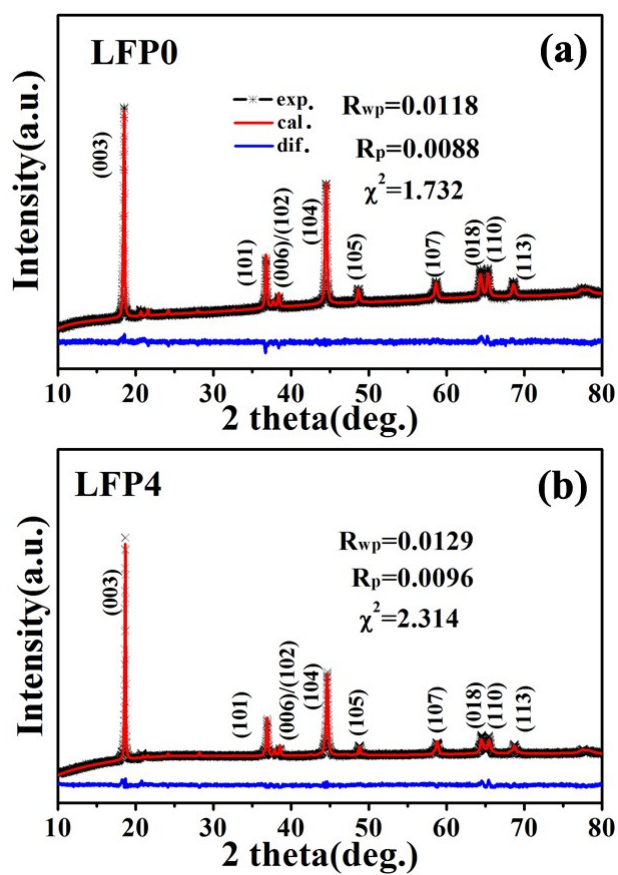


**Figure S1.** Calculated XRD patterns and corresponding reliability factors of the uncoated and coated samples: (a) LFP0 and (b) LFP4.

**Table S1.** Rietveld refinement atomic coordinates for sample LFP0 based on the XRD data.

| Atom            | Wyck position | x        | y        | z        | Occupancy |
|-----------------|---------------|----------|----------|----------|-----------|
| Li <sub>1</sub> | 3b            | 0.000000 | 0.000000 | 0.500000 | 0.9739    |
| Ni <sub>2</sub> | 3b            | 0.000000 | 0.000000 | 0.500000 | 0.0261    |
| Li <sub>2</sub> | 3a            | 0.000000 | 0.000000 | 0.000000 | 0.0261    |
| Ni <sub>1</sub> | 3a            | 0.000000 | 0.000000 | 0.000000 | 0.3069    |
| Co <sub>1</sub> | 3a            | 0.000000 | 0.000000 | 0.000000 | 0.3330    |
| Mn <sub>1</sub> | 3a            | 0.000000 | 0.000000 | 0.000000 | 0.3330    |
| O <sub>1</sub>  | 6c            | 0.000000 | 0.000000 | 0.260300 | 1.0000    |

**Table S2.** Rietveld refinement atomic coordinates for sample LFP4 based on the XRD data.

| Atom            | Wyck position | x        | y        | z        | Occupancy |
|-----------------|---------------|----------|----------|----------|-----------|
| Li <sub>1</sub> | 3b            | 0.000000 | 0.000000 | 0.500000 | 0.9774    |
| Ni <sub>2</sub> | 3b            | 0.000000 | 0.000000 | 0.500000 | 0.0226    |
| Li <sub>2</sub> | 3a            | 0.000000 | 0.000000 | 0.000000 | 0.226     |
| Ni <sub>1</sub> | 3a            | 0.000000 | 0.000000 | 0.000000 | 0.3104    |
| Co <sub>1</sub> | 3a            | 0.000000 | 0.000000 | 0.000000 | 0.3330    |
| Mn <sub>1</sub> | 3a            | 0.000000 | 0.000000 | 0.000000 | 0.3330    |
| O <sub>1</sub>  | 6c            | 0.000000 | 0.000000 | 0.261284 | 1.0000    |

**Table S3.** Lattice parameters of the samples refined by GSAS.

| Sample | Lattice parameters |              |            |                            |
|--------|--------------------|--------------|------------|----------------------------|
|        | <i>a</i> (Å)       | <i>c</i> (Å) | <i>c/a</i> | <i>V</i> (Å <sup>3</sup> ) |
| LFPO   | 2.8455(4)          | 14.219(8)    | 4.997      | 115.14(0)                  |
| LFP4   | 2.8512(2)          | 14.249(7)    | 4.997      | 115.84(2)                  |

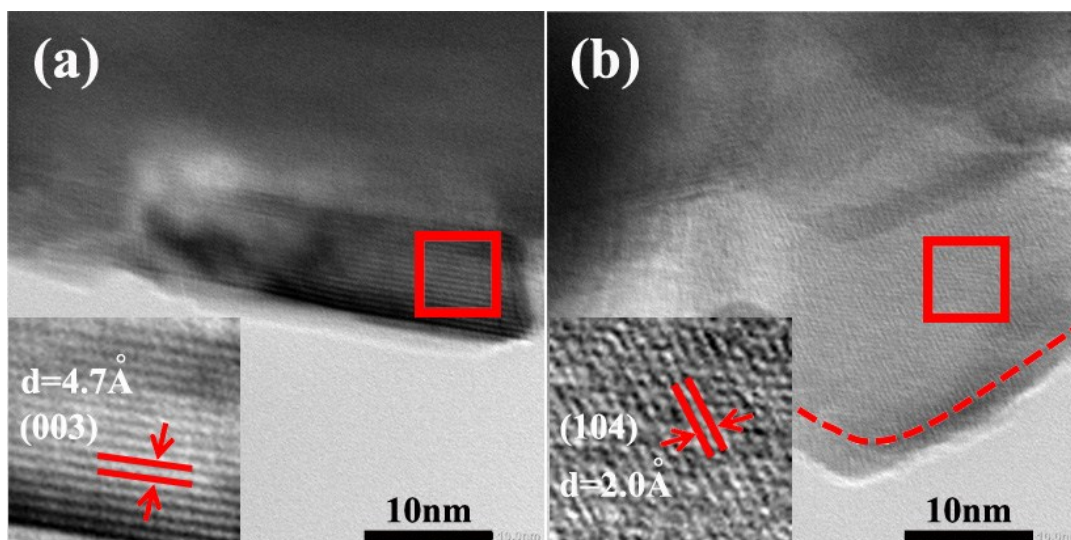


**Figure S2.** HRTEM images of the samples: (a) LFP0, (b) LFP4.

The HRTEM images of uncoated and  $\text{LiF/Li}_x\text{PF}_y\text{O}_z$ -coated  $\text{Li}_{1.2}\text{Mn}_{0.54}\text{Co}_{0.13}\text{Ni}_{0.13}\text{O}_2$  have been shown in Figure S2. As shown in the insets of Figure S2a and S2b, the lattice spacings are  $4.7\text{ \AA}$  for sample LFP0 and  $2.0\text{ \AA}$  for sample LFP4, which are coincided with the planes (003) and (104) of  $\text{LiMO}_2$ , respectively. These results (including the results of Figure 3) demonstrate that sample LFP0 and LFP4 are both composed of  $\text{Li}_2\text{MnO}_3$  and  $\text{LiMO}_2$  components.

**Table S4.** A comparison of electrochemical properties with literatures.

| Synthesis of<br>Li-rich | Samples   | Cycle / mAhg <sup>-1</sup>  | Reference          |
|-------------------------|---|---|--------------------|
| co-precipitation        | Ce <sub>0.8</sub> Sn <sub>0.2</sub> O <sub>2-s</sub> coated<br>Li <sub>1.2</sub> Mn <sub>0.54</sub> Ni <sub>0.13</sub> Co <sub>0.13</sub> O <sub>2</sub>                                  | 0.1C/238.1 mAhg <sup>-1</sup> /100 cycles/81.2%   | Ref.1 <sup>1</sup> |
| sol-gel                 | Li <sub>1.4</sub> Al <sub>0.4</sub> Ti <sub>1.6</sub> (PO <sub>4</sub> ) <sub>3</sub> coated<br>Li <sub>1.2</sub> Mn <sub>0.54</sub> Ni <sub>0.13</sub> Co <sub>0.13</sub> O <sub>2</sub> | 0.2C/192.4 mAhg <sup>-1</sup> /100 cycles /86.2%  | Ref.2 <sup>2</sup> |
| co-precipitation        | ZrO <sub>2</sub> coated<br>Li <sub>1.2</sub> Mn <sub>0.54</sub> Ni <sub>0.13</sub> Co <sub>0.13</sub> O <sub>2</sub>  | 0.2C/213.97 mAhg <sup>-1</sup> /100 cycles/ 86.7%   | Ref.3 <sup>3</sup> |
| sol-gel                 | Li <sub>3</sub> VO <sub>4</sub> coated<br>Li <sub>1.18</sub> Ni <sub>0.15</sub> Co <sub>0.15</sub> Mn <sub>0.52</sub> O <sub>2</sub>  | 4C/126.2 mAhg <sup>-1</sup> /100 cycles/78.6%   | Ref.4 <sup>4</sup> |
| co-precipitation        | Li <sub>2</sub> SiO <sub>3</sub> coated<br>Li <sub>1.2</sub> Ni <sub>0.13</sub> Co <sub>0.13</sub> Mn <sub>0.54</sub> O <sub>2</sub>  | 1C/142 mAhg <sup>-1</sup> /100 cycles /85.1%  | Ref.5 <sup>5</sup> |
| co-precipitation        | Li <sub>2</sub> ZrO <sub>3</sub> coated<br>Li <sub>1.2</sub> Ni <sub>0.13</sub> Co <sub>0.13</sub> Mn <sub>0.54</sub> O <sub>2</sub>  | 0.5C/225 mAhg <sup>-1</sup> /100 cycles/85%   | Ref.6 <sup>6</sup> |
| co-precipitation        | Li <sub>3</sub> PO <sub>4</sub> coated<br>Li <sub>1.2</sub> Ni <sub>0.13</sub> Co <sub>0.13</sub> Mn <sub>0.54</sub> O <sub>2</sub>   | 1C/214.5 mAhg <sup>-1</sup> /100 cycles/87.9%   | Ref.7 <sup>7</sup> |
| sol-gel                 | Fe <sub>2</sub> O <sub>3</sub> coated<br>Li <sub>1.2</sub> Ni <sub>0.2</sub> Mn <sub>0.6</sub> O <sub>2</sub>   | 0.1C/274 mAhg <sup>-1</sup> /50cycle/84%<br>1C/230 mAhg <sup>-1</sup> /100 cycles/80%   | Ref.8 <sup>8</sup> |
| co-precipitation        | LiF/Li <sub>x</sub> PF <sub>y</sub> O <sub>z</sub> coated<br>Li <sub>1.2</sub> Ni <sub>0.13</sub> Co <sub>0.13</sub> Mn <sub>0.54</sub> O <sub>2</sub>                                    | 0.1C/294.1 mAhg <sup>-1</sup> /50cycle/93.3%<br>0.5C/236 mAhg <sup>-1</sup> /100cycle/90.7%<br>1C/232.1 mAhg <sup>-1</sup> /100cycle/89.7%<br>2C/193.7 mAhg <sup>-1</sup> /100 cycle/91.8%<br>5C/188 mAhg <sup>-1</sup> /100cycle/91.2% | This<br>work       |

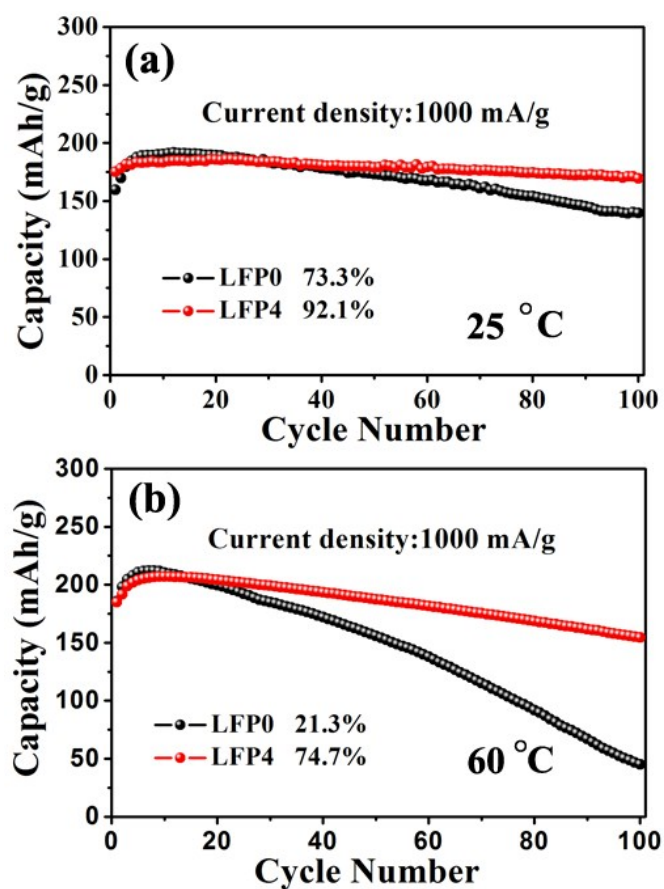


**Figure S3.** Cycle performances for the uncoated and LiF/Li<sub>x</sub>PF<sub>y</sub>O<sub>z</sub>-coated samples at the different temperature.

As shown in Figure S3a, at the same current density of 1000 mA/g at 25 °C, the initial discharge capacities were 159.7 mAh/g for sample LFP0 and 175.2 mAh/g for sample LFP4, respectively. After 100 cycles, the discharge capacities were 139.5 mAh/g for sample LFP0 and 169.5 mAh/g for sample LFP4, while the corresponding capacity retention ratios to the highest discharge capacities among 100 cycles were 73.3% for sample LFP0 and 92.1% for sample LFP4, respectively.

As shown in Figure S3b, at the same current density of 1000 mA/g at 60 °C, the initial discharge capacities were 185.5 mAh/g for sample LFP0 and 184.9 mAh/g for sample LFP4, respectively. After 100 cycles, the discharge capacities were 45.2 mAh/g for sample LFP0 and 154.3 mAh/g for sample LFP4, while the corresponding capacity retention ratios to the highest discharge capacities among 100 cycles were 21.3% for sample LFP0 and 74.1% for sample LFP4, respectively. These results further indicate that LiF/Li<sub>x</sub>PF<sub>y</sub>O<sub>z</sub> coated layer can significantly improve the cycling stability and inhibit the dissolution of metal ions causing by HF.

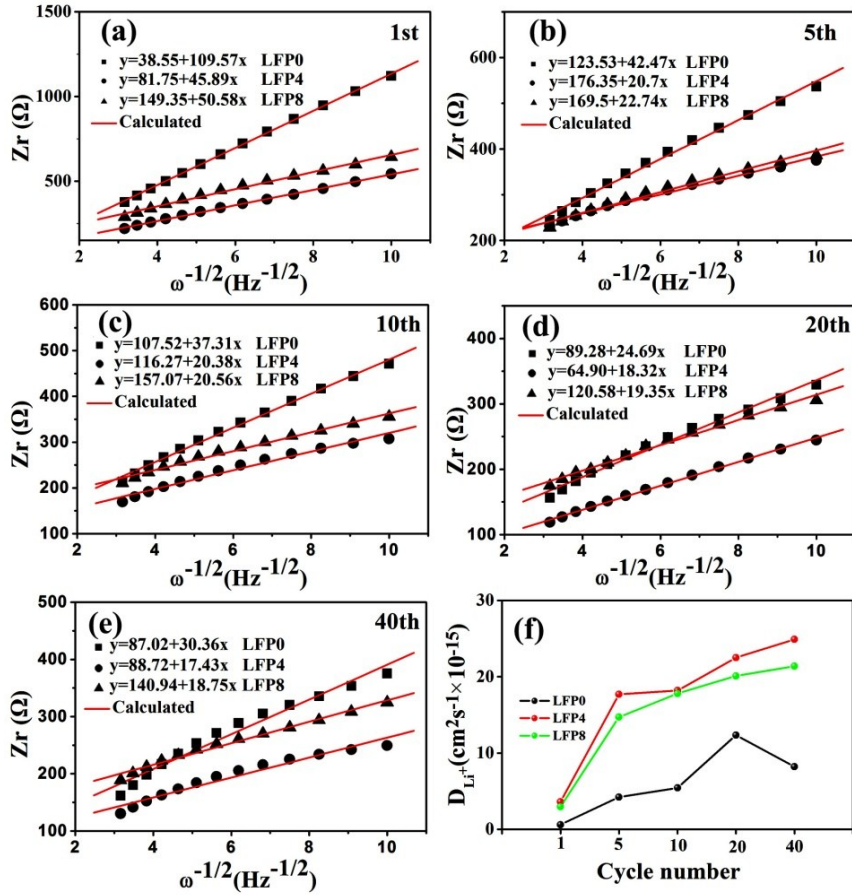


**Figure S4.** Profiles of the real parts of impedance ( $Z_r$ ) vs.  $\omega^{-1/2}$  from 0.1 to 0.01 Hz and corresponding linear fitting curves for samples LFP0, LFP4, and LFP8 at different cycles: (a) 1<sup>st</sup> cycle, (b) 5<sup>th</sup> cycle, (c) 10<sup>th</sup> cycle, (d) 20<sup>th</sup> cycle, and (e) 40<sup>th</sup> cycle. (f) Comparing for variations of Li-ion diffusion coefficients at different cycles for samples LFP0, LFP4, and LFP8.

The diffusion coefficient of lithium ion ( $D_{Li^+}$ ) is calculated from the straight sloping line at low frequency region (0.1-0.01Hz) according to the following equation<sup>9</sup>,

$$D_{Li^+} = \frac{0.5R^2T^2}{n^4 A^2 F^4 C^2 \sigma^2} \quad (1)$$

where R is the ideal gas content, T is the absolute temperature, n is the number of electron(s) per molecule oxidized, A is the surface area of the electrode, F is the Faraday constant, C is the concentration of  $Li^+$  in the cathode, and  $\sigma$  is the Warburg factor which has the relationship with  $Z_r$  as in the following equation,

$$Z_r = R_e + R_{sf} + R_{ct} + \sigma\omega^{-1/2} \quad (2)$$

From eqn.(2), the Warburg factor ( $\sigma$ ) can be obtained from the linear fitting of  $Z_r$  vs.  $\omega^{-1/2}$ , as shown in Figure S1. The calculated results of lithium diffusion coefficients at different cycles for samples LFP0, LFP4, and LFP8 were exhibited in Table S5.

**Table S5.** Fitted parameters of EIS data for sample LFP0, LFP4, and LFP8 at different cycles.

| Sample | Cycle            | $R_e(\Omega)$ | $R_{sf}(\Omega)$ | $R_{ct}(\Omega)$ | $R_{total}(\Omega)$ | $D_{Li^+}(cm^2s^{-1})$ |
|--------|------------------|---------------|------------------|------------------|---------------------|------------------------|
| LFP0   | 1 <sup>st</sup>  | 2.87          | 82.43            | 2012.0           | 2097.3              | $6.29*10^{-16}$        |
|        | 5 <sup>th</sup>  | 2.98          | 60.83            | 1318.1           | 1381.9              | $4.2*10^{-15}$         |
|        | 10 <sup>th</sup> | 3.20          | 28.74            | 425.9            | 457.8               | $5.43*10^{-15}$        |
|        | 20 <sup>th</sup> | 3.67          | 19.41            | 250.1            | 273.2               | $1.24*10^{-14}$        |
|        | 40 <sup>th</sup> | 3.49          | 14.21            | 428.0            | 445.7               | $8.20*10^{-15}$        |
|        | 60 <sup>th</sup> | 3.60          | 19.94            | 988.2            | 1011.7              | --                     |
| LFP4   | 1 <sup>st</sup>  | 2.63          | 50.75            | 884.7            | 938.1               | $3.59*10^{-15}$        |
|        | 5 <sup>th</sup>  | 2.75          | 45.76            | 510.4            | 558.9               | $1.77*10^{-14}$        |
|        | 10 <sup>th</sup> | 2.84          | 38.43            | 307.9            | 349.2               | $1.82*10^{-14}$        |
|        | 20 <sup>th</sup> | 2.98          | 10.34            | 216.9            | 230.2               | $2.25*10^{-14}$        |
|        | 40 <sup>th</sup> | 3.02          | 8.21             | 243.5            | 254.7               | $2.49*10^{-14}$        |
|        | 60 <sup>th</sup> | 3.10          | 8.43             | 391.8            | 403.3               | --                     |
| LFP8   | 1 <sup>st</sup>  | 2.76          | 67.83            | 974.5            | 1045.1              | $2.97*10^{-15}$        |
|        | 5 <sup>th</sup>  | 2.88          | 73.57            | 523.6            | 600.1               | $1.47*10^{-14}$        |
|        | 10 <sup>th</sup> | 3.13          | 68.03            | 417.7            | 488.9               | $1.78*10^{-14}$        |
|        | 20 <sup>th</sup> | 3.25          | 40.05            | 352.0            | 395.3               | $2.01*10^{-14}$        |
|        | 40 <sup>th</sup> | 3.40          | 35.31            | 340.2            | 378.9               | $2.14*10^{-14}$        |
|        | 60 <sup>th</sup> | 3.55          | 37.99            | 576.0            | 617.5               | --                     |

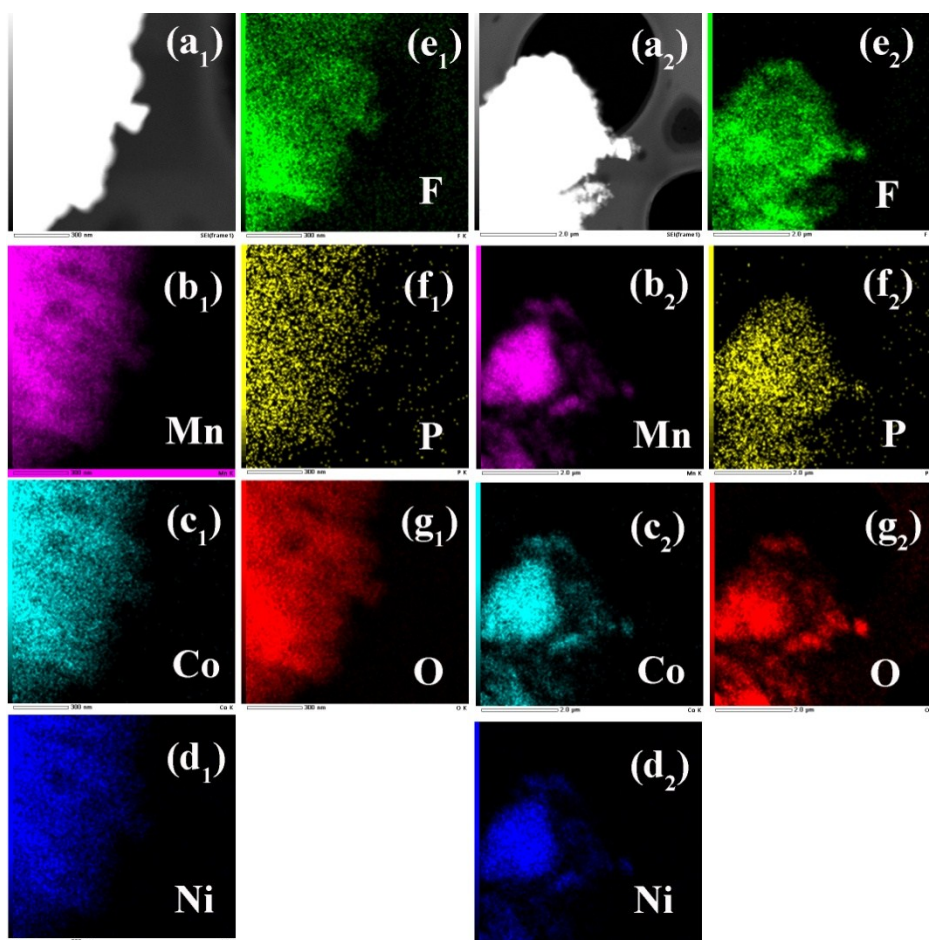


**Figure S5.** EDX-mapping images of electrodes after 60cycles for the samples: (a<sub>1</sub>-g<sub>1</sub>) LPF0, (a<sub>2</sub>-g<sub>2</sub>) LPF4 .

**Table S6** The molar ratios of Mn, Co, Ni elements for sample LFP0 and LFP4 obtained by EDX-mapping from TEM measurements.

|      | Sample                  | Mn   | Co    | Ni    |
|------|-------------------------|------|-------|-------|
| LFP0 | Fresh powder            | 0.54 | 0.138 | 0.137 |
|      | Eletrode after 60 cycle | 0.54 | 0.120 | 0.104 |
| LFP4 | Fresh powder            | 0.54 | 0.135 | 0.131 |
|      | Eletrode after 60 cycle | 0.54 | 0.128 | 0.112 |

The molar ratios of Mn, Co, Ni elements for sample LFP0 and LFP4 were compared through measuring the EDX-mapping from TEM. As shown in Table S6, the dissolutions of Co and Ni elements for uncoated sample LFP0 are more than those of coated sample LFP4 when the content of Mn is fixed at 0.54. If Mn element also dissolves, the Co and Ni elements should dissolve even more for uncoated sample LFP0. All these results indicate that the coating layer can suppress the dissolution of transition metal ions.

## Reference

1. Y. Liu, Z. Yang, J. Li, B. Niu, K. Yang and F. Kang, *J. Mater. Chem. A*, 2018, **6**, 13883-13893.
2. D. Gao, Z. Zeng, H. Mi, L. Sun, X. Ren, P. Zhang and Y. Li, *J. Mater. Chem. A*, 2019, DOI: 10.1039/C9TA04551A.
3. J. C. Zheng, Z. Yang, P. B. Wang, L. B. Tang, C. S. An and Z. J. He, *ACS Appl. Mater. Interfaces*, 2018, **10**, 31324-31329.
4. Q. Fu, F. Du, X. Bian, Y. Wang, X. Yan, Y. Zhang, K. Zhu, G. Chen, C. Wang and Y. Wei, *J. Mater. Chem. A*, 2014, **2**, 7555-7562.
5. L. Zhou, Y. Wu, J. Huang, X. Fang, T. Wang, W. Liu, Y. Wang, Y. Jin and X. Tang, *J. Alloy. Comp.*, 2017, **724**, 991-999.
6. K. R. Prakasha, M. Sathish, P. Bera and A. S. Prakash, *ACS Omega*, 2017, **2**, 2308-2316.
7. M.-J. Wang, F.-D. Yu, G. Sun, J. Wang, J.-G. Zhou, D.-M. Gu and Z.-B. Wang, *J. Mater. Chem. A*, 2019, **7**, 8302-8314.
8. S. Chen, Y. Zheng, Y. Lu, Y. Su, L. Bao, N. Li, Y. Li, J. Wang, R. Chen and F. Wu, *ACS Appl. Mater. Interfaces*, 2017, **9**, 8669-8678.
9. C. Fu, G. Li, D. Luo, J. Zheng and L. Li, *J. Mater. Chem. A*, 2014, **2**, 1471-1483.